Available online at www.sciencedirect.com

ScienceDirect

journal homepage: www.elsevier.com/locate/bbe

Original Research Article

Modelling and control of a failing heart managed by a left ventricular assist device☆

Jeongeun Son [a], *Dongping Du* [b], *Yuncheng Du* [a,*]

[a] *Department of Chemical & Biomolecular Engineering, Clarkson University, Potsdam, NY, USA*
[b] *Department of Industrial, Manufacturing & Systems Engineering, Texas Tech University, Lubbock, TX, USA*

ARTICLE INFO

Article history:
Received 8 November 2019
Received in revised form
28 December 2019
Accepted 27 January 2020
Available online 20 February 2020

Keywords:
Self-tuning controller
Cardiovascular modelling
Left ventricular assist device control
Uncertainty quantification
Optimization

ABSTRACT

Left ventricular assist device (LVAD) recently has been used in advanced heart failure (HF), which supports a failing heart to meet blood circulation demand of the body. However, the pumping power of LVADs is typically set as a constant and cannot be freely adjusted to incorporate blood need from resting or mild exercise such as walking stairs. To promote the adoption of LVADs in clinical use as a long-term treatment option, a feedback controller is needed to regulate automatically the pumping power to support a time-varying blood demand, according to different physical activities. However, the tuning of pumping power induces suction, which will collapse the heart and cause sudden death. It is essential to consider suction when developing control strategy to adjust the pumping power. Further, hemodynamic of a failing heart exhibits variability, due to patient-to-patient heterogeneity and inherent stochastic nature of the heart. Such variability poses challenges for controller design. In this work, we develop a feedback controller to adjust the pumping power of an LVAD without inducing suction, while incorporating variability in hemodynamic. To efficiently quantify variability, the generalized polynomial chaos (gPC) theory is used to design a robust self-tuning controller. The efficiency of our control algorithm is illustrated with three case scenarios, each representing a specific change in physical activity of HF patients.

1. Introduction

Heart failure (HF) is a critical condition that a failing heart cannot eject appropriate amount of blood and oxygen to maintain the body healthy. The well-known therapy for severe HF is transplant [1]; but only about 5000 patients per year worldwide can receive transplants, due to limited donor hearts. Larger numbers of patients are eligible for transplants, but about 30% of them die while waiting for donor hearts [2]. As an alternative, mechanical assist devices, e.g., Left Ventricular Assist Devices (LVAD), have been used in clinical practice to support a failing heart either before a donor heart is available or until cardiomyocyte function recovers [1,3].

In clinical practices, the pumping power of an LVAD is set up typically by physicians with knowledge gleaned in surgery,

☆ This paper was partially presented at the 2019 American Control Conference (ACC), Philadelphia, PA, USA, July 10–12, 2019.

* *Corresponding author at*: Department of Chemical & Biomolecular Engineering, Clarkson University, Potsdam, NY, USA
E-mail address: ydu@clarkson.edu (Y. Du).

https://doi.org/10.1016/j.bbe.2020.01.014

which cannot be adjusted afterwards [4,5]. But the physiological demand of blood changes with respect to various physical activities—resting or mild exercising such as walking stairs. To meet a time-varying blood demand, it is essential to automatically adjust the pumping power of an LVAD.

One challenge to adjust the pumping power is to avoid suction. When the pumping power is increased above a certain limit, it will induce ventricular suction, which is a state that the pump seeks to draw out more blood from the left ventricle than the available blood in it [4]. Suction will collapse the heart and consequently cause sudden death. Of paramount importance is to develop robust controllers to automatically adjust the pump speed with respect to time-varying physical activity to satisfy blood demands, while preventing the ventricular suction. Several control algorithms have been previously reported [4,6–11], and each addresses a particular issue for the tuning of the pumping power of an LVAD.

In addition, the activity level of HF patients is very limited [12], since the blood supplied with constant pump speed cannot meet perfusion demand during even mild exercise, e.g., walking stairs. To address this, controllers were developed to adjust pumping speed. For example, the value of the systemic vascular resistance (SVR) in a model was used to describe different levels of physical activities for controller design [2,13–15]. But the right heart, including the right atrium and ventricle, and the pulmonary circulation, were often assumed to be strong and healthy, thus their effects on the tuning of pumping speed were not studied. Importantly, as the activity level changes, hemodynamics of the right heart and pulmonary circulation, e.g., the right ventricle contractility and the pulmonary vascular resistance, will vary [4]. Thus, it is essential to consider these hemodynamic parameters, while developing control strategy to adjust the pumping speed. Notably, parameters such as the SVR are often assumed to be given a priori for control design in existing works. However, values of these parameters cannot be known with certainty, since the heart condition of the same patient varies over time and since there is heterogeneity among individual HF patients. These will introduce uncertainty, which will affect the control design and deteriorate the control performance.

To address the challenges noted above, a detailed model of the heart managed by an LVAD is first presented in this work, which includes both the left and right sides of the heart. Using the model, a robust control algorithm is developed to adjust the pumping speed of an LVAD to account for different physical activities, while preventing suction. To consider the effect of the inter-and/or intra-patient uncertainty on the controller design, uncertainty analysis (UA) technique is used in this work [16].

Monte Carlo (MC) simulation is the most popular tool for UA since it only requires repetitive executions of models with various samples of uncertainty. However, MC is computationally prohibitive, since it requires larger number of samples to ensure UA accuracy. To alleviate the computational burden, generalized polynomial chaos (gPC) expansion can be used, which has shown its efficiency in several modelling, control, and optimization problems [17–21]. Compared to MC, gPC mathematically approximates an uncertainty with an analytical expression and further efficiently quantify its effect on model predictions in real time [22]. Since our objective is to rapidly adjust the pumping speed to meet blood need for time-varying physical activity, gPC is thus used for controller design, due to its computational efficacy.

Specifically, in this work the controller will adjust the pumping speed to provide appropriate blood without inducing suction, while considering uncertainty in hemodynamic parameters (e.g., SVR), which are related to different physical activities. In summary, contributions in this work include: (i) development of a stochastic cardiovascular model managed by an LVAD based on existing models in the literature; (ii) implementation of the gPC to efficiently quantify the impact of parametric uncertainty on model predictions (e.g., pump flow) that are essential for LVAD control; (iii) formulation of an optimization problem to identify the most favourable controller parameters, such that the LVAD can appropriately adjust the pumping speed without inducing suction; and (iv) the design of a self-tuning controller to regulate the pumping speed of an LVAD and to quickly bring it back to a safe operating condition under suction, resulting from unexpected and sudden changes in heart condition of subjects.

This paper is organized as follows. Section 2 presents a deterministic nonlinear model of a failing heart managed by an LVAD and the theoretical background of gPC. Details of the control algorithm are given in Section 3, followed by results of computer experiments and a brief discussion in Sections 4 and 5, respectively. Conclusions are given in Section 6.

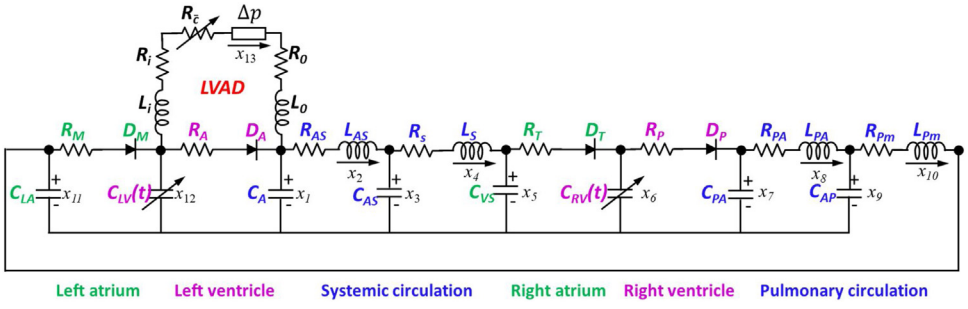

Fig. 1 – Schematic of the deterministic model of a failing heart managed by an LVAD. The presentation of the deterministic model is based on existing works in the literature [2,4,9,14,23,24].

2. Theoretical background

2.1. Cardiovascular-LVAD model

Based on existing works [2,4,9,14,23,24], a model is first presented to describe the cardiovascular system supported by an LVAD, which is a comprehensive combination of models noted above. For example, the right heart is considered, as compared to previous works [2,14], where the right heart was assumed to be healthy and was not included in the model. Compared to the model of Fernandez de Canete et al. [24], the effect of an LVAD on the failing heart is studied. Also the ''double hill'' function is used to describe the contractility of the heart in order to reduce model complexity, compared to other works in Refs. [4,9,23,24]. Note that other elastance models can be used to describe elastance properties based on systole and diastole periods [23,24] or based on ECG signals [25–27], but it is not considered here for brevity.

Fig. 1 shows a schematic of the equivalent circuit model; and Table 1 lists its corresponding state variables used in the model, for which model parameters are defined with fixed constants as in Table 2. It is important to note that the model is hereafter referred to as deterministic models, compared to the stochastic model developed in the results section, for which model parameters will be described by probability density function (PDF) rather than a constant.

The deterministic model in Fig. 1 is described by the systemic and pulmonary circulations, left atrium (LA), left ventricle (LV), right atrium (RA), and right ventricle (RV). In each cardiac cycle, blood leaves the pulmonary circulation and flows into the LA, and then flows into the LV via mitral valve (D_M). Due to heart contraction and mechanical supports of an LVAD, the blood is ejected into the systemic circulation via the aortic valve (D_A) and LVAD simultaneously.

Once the blood has supplied the body with oxygen and nutrients, it returns the deoxygenated blood into RA, RV, and the pulmonary system by passing through the tricuspid (D_T) and the pulmonary (D_P) valves. The pulmonary circulation in Fig. 1 is described by the pulmonary artery and arterial pulmonary compliances (C_{PA} & C_{AP}), resistances (R_{PA} & R_{Pm}), and inertances (L_{PA} & L_{Pm}). Similarly, compliances (C_A & C_{AS}), resistances (R_{AS} & R_S), and inertances (L_{AS} & L_S) are used to describe the systemic circulation [9]. Following the literature [2,13,14], the systemic vascular resistance (SVR), i.e., R_S in Fig. 1, is used to describe physical activity in this work. For example, when a HF patient implanted with an LVAD starts to exercise, e.g., walking stairs, the value of R_S will be decreased. Similarly, pulmonary vascular resistance (PVR), i.e., R_{Pm} in Fig. 1, is another variable considered here to describe different levels of physical activity. For example, PVR (or R_{Pm}) decreases as the patient becomes more active, e.g., from resting to mild exercise [4,15]. Further, the contractility of both ventricles is defined with the reciprocal of C_{RV} and C_{LV}, respectively [14,28,29], which are also used to define physical activity. As the literature reported [4], the contractility of both ventricles increases as the patients become more active.

In addition, resistors, i.e., R_A, R_M, R_T, and R_P in Fig. 1, are used to describe the aortic valve, mitral valve, tricuspid valve, and pulmonary valve, respectively. The diodes, i.e., D_M, D_A, D_T, and D_P, describe dynamic behaviors of valves with respect to four separated phases of a cardiac cycle, e.g., the isovolumic relaxation, filling, isovolumic contraction, and ejection [14].

Further, R_i, R_o, L_i, and L_o in Fig. 1 are the resistances and inertances of the inflow and outflow of the pump cannulas, and suction is mathematically defined with the suction resistance R_c as follows [9]:

$$R_c = \begin{cases} 0, & if\ LVP(t) > LVP \\ -3.5(LVP(t) - LVP), & otherwise \end{cases} \quad (1)$$

where LVP is the threshold of the LV, which is set to 1 $mmHg$. Details of each model parameter can be found in the literature [2,4,9,14,23,24].

For time-varying compliances in Fig. 1, i.e., $C_{LV}(t)$ and $C_{RV}(t)$, their inverse is defined as the elastance function to describe the contractility of each ventricle, which is defined as a function of pressure and volume in each ventricle as below [14,28–30]:

$$E(t) = \frac{1}{C(t)} = \frac{VP(t)}{VV(t) - V_0} \quad (2)$$

where $VP(t)$ is the pressure of the left or right ventricles, i.e., x_6 or x_{12} in Table 1, $VV(t)$ and V_0 are the time-varying ventricular

Table 1 – Variables used in the deterministic model of the heart managed by an LVAD. Description of model variables follows similar definition as noted in previous works [2,4,9,14,23,24].

Variables	Physiological meaning (definition)	Units
$x_1(t)$, $AoP(t)$	Aortic pressure	$mmHg$
$x_2(t)$, $Q_{AS}(t)$	Arterial systemic circulation blood flow	ml/s
$x_3(t)$, $ASP(t)$	Arterial systemic pressure	$mmHg$
$x_4(t)$, $Q_{VS}(t)$	Venous systemic circulation blood flow	ml/s
$x_5(t)$, $RAP(t)$	Right venous-atrial pressure	$mmHg$
$x_6(t)$, $RVP(t)$	Right ventricular pressure	$mmHg$
$x_7(t)$, $PAP(t)$	Pulmonary artery pressure	$mmHg$
$x_8(t)$, $Q_{AP}(t)$	Arterial pulmonary circulation blood flow	ml/s
$x_9(t)$, $APP(t)$	Arterial pulmonary pressure	$mmHg$
$x_{10}(t)$, $Q_{VP}(t)$	Venous pulmonary circulation blood flow	ml/s
$x_{11}(t)$, $LAP(t)$	Left venous-atrial pressure	$mmHg$
$x_{12}(t)$, $LVP(t)$	Left ventricular pressure	$mmHg$
$x_{13}(t)$, $Q_P(t)$	LVAD Pump flow	ml/s

Table 2 – Description of model parameters and their values used in the cardiovascular-LVAD model. Description and values of model parameters follow previously reported work in the literature [2,4,9,14,23,24].

Parameter	Physiological meaning/definition (Units)	Values
R_{AS}	Aortic-systemic resistance (mmHg·s/ml)	0.03980
R_S	Systemic vascular resistance (mmHg·s/ml)	1.00000
R_T	Tricuspid valve resistance (mmHg·s/ml)	0.00500
R_P	Pulmonary valve resistance (mmHg·s/ml)	0.00100
R_{PA}	Pulmonary artery resistance (mmHg·s/ml)	0.03376
R_{Pm}	Pulmonary vascular resistance (mmHg·s/ml)	0.10100
R_M	Mitral valve resistance (mmHg/ml/s)	0.00500
R_A	Aortic valve resistance (mmHg/ml/s)	0.00100
R_i	Inlet resistance of cannulae (mmHg/ml/s)	0.06770
R_o	Outlet resistance of cannulae (mmHg/ml/s)	0.06770
R_c	Suction Resistance (mmHg/ml/s)	Eq. (1)
L_{AS}	Aortic-systemic inertance (mmHg·s^2/ml)	0.00050
Ls	Systemic inertance (mmHg·s^2/ml)	0.00360
L_{PA}	Pulmonary artery inertance (mmHg·s^2/ml)	0.00075
L_{Pm}	Pulmonary inertance (mmHg·s^2/ml)	0.00308
L_i	Inlet inertance of cannulae (mmHg·s^2/ml)	0.01270
L_o	Outlet inertance of cannulae (mmHg·s^2/ml)	0.01270
C_A	Aortic compliance (ml/mmHg)	0.08000
C_{AS}	Arterial systemic compliance (ml/mmHg)	1.33000
C_{VS}	Venous systemic compliance (ml/mmHg)	7.50000
C_{RV}	Right ventricular compliance (ml/mmHg)	Time-varying
C_{PA}	Pulmonary artery compliance (ml/mmHg)	0.03270
C_{AP}	Arterial pulmonary compliance (ml/mmHg)	2.67000
C_{VP}	Venous pulmonary compliance (ml/mmHg)	4.40000
C_{LV}	Left ventricular compliance (ml/mmHg)	Time-varying
D_T	Tricuspid valve	–
D_P	Pulmonary valve	–
D_M	Mitral valve	–
D_A	Aortic valve	–

volume and the theoretical volume of the left or right ventricles with a pressure of 0 *mmHg*, respectively. In (2), $E(t)$ is further defined as in [2,14,31]:

$$E(t) = (E_{max} - E_{min})E_n(t_n) + E_{min} \tag{3}$$

$$E_n(t_n) = 1.55\left[\frac{\left(\frac{t_n}{0.7}\right)^{1.9}}{1+\left(\frac{t_n}{0.7}\right)^{1.9}}\right]\left[\frac{1}{1+\left(\frac{t_n}{1.17}\right)^{21.9}}\right] \tag{4}$$

where $E_n(t_n)$ is the normalized elastance function, which is often referred to as ''double hill'' function [31]; and E_{max} and E_{min} are the maximum and the minimum elastance in the systole and diastole, respectively. Notably, E_{max} can be altered to define different physical activities [4].

In addition, t_n in (3) and (4) is defined as: $t_n = t_m/t_p$, where t_m is the time period calculated with modular arithmetic function as: t_m = mod(t, t_c), and t_c is the cardiac cycle that is the reciprocal of the heart rate (*HR*, *beat per minute or bpm*). Also, t_p is the time to reach the peak elastance, depending the ratio of the systole to diastole of a patient and HR [4,31]. It is important to note that the ratio of t_p to t_c is fixed in this work to maintain a constant ratio between the systolic and diastolic periods in each cardiac cycle.

In addition, the pressure difference Δp across an LVAD, i.e., the difference between the LV pressure (LVP, x_{12}) and aortic pressure (AoP, x_1), can be described as in [2,32]:

$$\begin{aligned}\Delta p &= \mathrm{LVP}(t) - \mathrm{AoP}(t)\\ &= (R_i + R_o + R_c + a_o)Q_P + (L_i + L_o + a_1)\frac{dQ_P}{dt} - a_2\omega^2\end{aligned} \tag{5}$$

where α_0, α_1, and α_2 are model parameters describing an LVAD. As others noted [2], α_0, α_1, and α_2 were set to 0.1707, 0.02177, and 9.9025e-07, respectively, which were calibrated to fit a totally implantable LVAD pump from the Nimbus Inc. in Rancho Cordova, CA.

In summary, the deterministic cardiovascular system with an LVAD can be described as in:

$$\dot{x} = A(t)x + B(t)b(x) + cu(t) \tag{6}$$

where $\boldsymbol{x}$ is a vector of 13 variables defined in Table 1, $\boldsymbol{A}(t)$ and $\boldsymbol{B}(t)$ are (13 × 13) and (13 × 4) time-varying matrices, $b(\boldsymbol{x})$ and c are (4 × 1) and (13 × 1) vectors, and u(t) is related to the pump speed $\omega(t)$, i.e., $u(t) = \omega^2(t)$, which will be tuned by a controller, explained below. Again, this model will be modified to build a stochastic model explained later, using the gPC theory.

2.2. *Generalized polynomial chaos (gPC) expansion*

To consider uncertainty (e.g., patient heterogeneity and variability in model parameters), the gPC expansion is used [16,22], which will convert the cardiovascular-LVAD model in

(6) into a number of coupled stochastic models. For illustration, we focus on parametric uncertainty and describe a model parameter with a probability density function (PDF) instead of a fixed value. For example, it is hypothesized that the exact value of SVR is unknown to modelers, but its PDF can be estimated or given by physicians. Following this, it can be approximated with a random variable with prescribed PDF in the Wiener-Askey theory [33].

For simplicity, we rewrite the deterministic cardiovascular-LVAD system in (6) as in:

$$\dot{x} = f(t, x, v, g; u) \tag{7}$$

where f represents nonlinear functions; $\boldsymbol{v}$ are fixed and constant model parameters; $\boldsymbol{g}$ are used to define parametric uncertainty (e.g., uncertain parameters such as SVR) that are described by PDFs; and $\boldsymbol{x}$ are state variables described in Table 1.

To evaluate the impact of uncertainty g on $\mathbf{x}$, the first step is to approximate each parameter in $\boldsymbol{g}$ with a random variable ξ. For example, (8) shows the gPC approximation of the SVR (R_S in Fig. 1) as follows [22]:

$$R_S(t, \xi) = \sum_{i=0}^{\infty} r_i(t)\psi_i(\xi) \approx \sum_{i=0}^{q} r_i(t)\psi_i(\xi) \tag{8}$$

where $\{r_i\}$ are appropriately selected gPC coefficients such that R_S follows *a priori* prescribed PDF, and $\{\psi_i(\xi)\}$ are polynomial basis functions, which are selected with respect to the PDF. For example, if R_S is normally distributed, the best choice of $\psi_i(\xi)$ is Hermite polynomial basis function [22,33].

Since uncertainty in $\boldsymbol{g}$ can affect $\mathbf{x}$, each variable in $\boldsymbol{x}$ is also estimated with ξ and polynomial basis functions $\Psi_l(\xi)$ as in [33]:

$$x_j(t, \xi) = \sum_{l=0}^{\infty} x_{j,l}(t)\Psi_l(\xi) \approx \sum_{l=0}^{Q} x_{j,l}(t)\Psi_l(\xi) \tag{9}$$

where $\{x_{j,l}\}$ are the gPC coefficients of the j^{th} variable in $\boldsymbol{x}$ at t. Notably, $\{x_{j,l}\}$ in (9) will be calculated by substituting (8) and (9) into the model (7) and by using a Galerkin projection. In this way, (7) is projected onto each basis function $\Psi_l(\xi)$ with an inner product as in [22]:

$$\langle \dot{x}(t, \xi), \Psi_l(\xi)\rangle = \langle f(t, x, v, g; u), \Psi_l(\xi)\rangle \tag{10}$$

This yields a set of coupled models to describe uncertainty in $\mathbf{x}$, e.g., variance in $\boldsymbol{x}$ resulting from uncertainty in $\boldsymbol{g}$. It is worth mentioning that finite numbers of terms, $q+1$ and $Q+1$ (including zeroth term) are often used in (8) and (9), instead of infinite number of terms. The number of terms in (9), i.e., $Q+1$, is calculated with a heuristic formula as below [33]:

$$Q + 1 = \frac{(n+q)!}{n!q!} \tag{11}$$

where q is the polynomial order in (8) required to estimate *a priori* known PDF of R_S, and n represents the number of uncertainties, which is set to 1 in this work, since only uncertainty in SVR (R_S) is considered.

The inner product in (10) is mathematically defined as in [33]:

$$\langle \varphi(\xi), \varphi'(\xi)\rangle = \int \varphi(\xi)\varphi'(\xi)W(\xi)d\xi \tag{12}$$

where the integral is calculated over the domain generated by all random variables ξ, and $W(\xi)$ is a weighting function, i.e., PDF of ξ, conditioned on polynomial basis functions [22].

When the gPC coefficients of $\boldsymbol{x}$ in (9) are obtained, the mean and variance of $\boldsymbol{x}$ at a given time point t can be rapidly estimated as follows [22]:

$$\begin{aligned} E[x_j(t)] &= E\left[\sum_{l=0}^{Q} \dot{x}_{j,l}(t)\psi_l\right] = \dot{x}_{j,0}(t)E[\psi_0] + \sum_{l=1}^{Q} \dot{x}_{j,l}(t)E[\psi_l] \\ &= \dot{x}_{j,0}(t) \end{aligned} \tag{13}$$

$$\begin{aligned} Var[x_j(t)] &= E\left[\{x_j(t) - E[x_j(t)]\}^2\right] \\ &= E\left[\left\{\sum_{l=0}^{Q} x_{j,l}(t)\Psi_l - x_{j,(l=0)}(t)\right\}^2\right] \end{aligned}$$

$$= E\left[\left\{\sum_{l=1}^{Q} x_{j,l}(t)\Psi_l\right\}^2\right] = \sum_{l=1}^{Q}\{x_{j,l}(t)\}^2 E[\Psi_l^2] \tag{14}$$

As seen, the mean and variance are related to different gPC coefficients. For example, the first coefficient is the mean value of $\mathbf{x}$, whereas the variance is calculated with higher order gPC coefficients [22]. Since the mean and variance can be calculated online, it motivates us to use the gPC and to integrate it with the deterministic model in Section 2.1 to develop a stochastic model of the cardiovascular-LVAD system for robust control design in this work.

3. Control design under uncertainty

3.1. *Parameters related to different physical activities*

For the deterministic cardiovascular-LVAD model in Section 2, five parameters can be used to describe the physical activity. These parameters are the heart rate (HR), the contractility of the left and right heart chambers (E_{max}), and the systemic vascular resistance (SVR or R_S in Fig. 1), and the pulmonary vascular resistance (PVR or R_{Pm} in Fig. 1). In this work, we focus on SVR (R_S), since it is closely related to the left ventricle afterload and the tuning of the pumping speed is more sensitive to changes in SVR, as reported in clinical studies [9,34]. Further, it is assumed that the exact value of R_S is unknown, but its PDF can be estimated, which describes the inter- and/or intra-patient uncertainty. Specifically, R_S has perturbations around the mean values given in Fig. 2, where the blue dash line shows two mean values and the solid line represents random perturbations around a specific mean value. Each mean value defines a particular level of physical

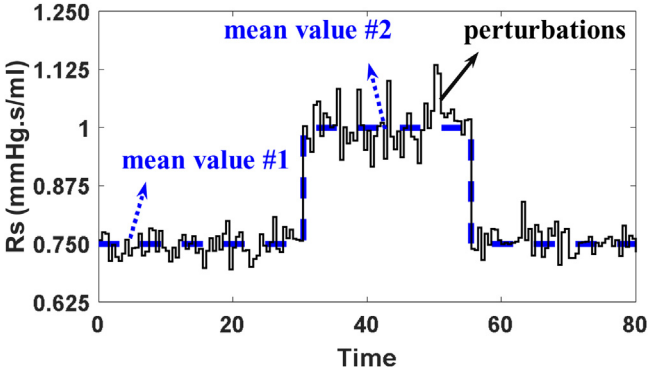

Fig. 2 – Diagram to illustrate a time-varying systemic vascular resistance (R_S, SVR) for two physical activity levels, following our previous work [16].

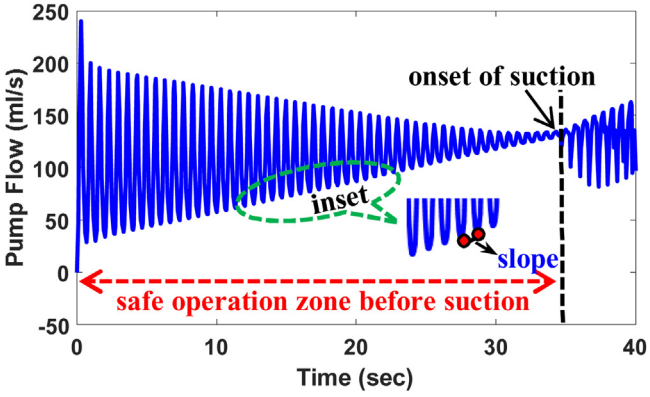

Fig. 3 – Dynamic changes in pump flow with a linearly increasing pump speed. For illustration, R_S in the model is set to 1.0 mmHg·s/ml, and the suction occurs when the pump speed reaches about 1.35×10^4 krpm [16].

activity. For example, 0.75 mmHg·s/ml is used to represent mild exercise and 1 mmHg·s/ml is used to define resting. The PDF of R_S is assumed to be available, since it can be determined by clinicians and the variation around the mean values is used to incorporate patient heterogeneity and model uncertainty.

In the presence of uncertainty in R_S, our objective is to tune the pumping speed with respect to changes in physical activity to satisfy different blood needs, while preventing suction. The controller of LVAD should adjust the pumping speed online using the available information. In this work, the pump flow is assumed to be available to identify an appropriate pumping speed, since it can be estimated with indirect techniques (e.g., contrast echocardiography) [35] in clinics or it can be calculated with the pump information (e.g., pump power or speed) and the pressure difference between the inflow and outflow of cannula [36]. This ensures the applicability of the control strategy in clinical practices for commercialized LVAD products.

3.2. *Relationship between pump flow and suction*

Since suction means the pump seeks to draw more blood out than the available one in the left ventricle, the pump flow is used as an indicator for suction detection. As others noted [2,37–39], there is a relationship between suction and pump flow. For example, Fig. 3 shows the simulation results of the pump flow under a linearly increasing pump speed over time. As can be seen, the pulsatility of the pump flow decreases as the pumping speed increases. Especially, the pulsatility is minimized when suction happens and then increases gradually after the onset of suction. Further, as literature reported [2], there is a sign change in the slope calculated by the minimum pump flow in consecutive cardiac cycles before and directly after the onset of suction. As can be observed in the inset of Fig. 3, the slope calculated with the pump flow is positive before suction happens. When the pumping speed increases, the pulsatility decreases gradually and approaches zero eventually. This speed can be defined as a *breakpoint*, at which if the pumping speed is further increased, suction will happen. In the presence of suction, the sign of the slope changes from positive to negative as can be observed in Fig. 3.

The pulsatility and the sign change of slopes provide useful information to adjust the pumping speed. It is important to note that the deterministic model of the cardiovascular-LVAD system was used for simulations in Fig. 3 to illustrate the relationship between the pump flow (i.e., Q_P in Table 1) and

suction. However, using the gPC as discussed in Section 2, it is possible to predict both the mean and variance of the pump flow under uncertainty in R_S. To capitalize on predictions, in this work the mean value of pump flow is used for suction prevention, whereas the variance is used as a criterion for *fine-tuning* of the controller parameter. This will be further discussed in the following sections.

3.3. Feedback controller design

Based on the discussion above, the tuning of pumping speed can be mathematically defined as in [2]:

$$\omega(z+1) = \omega(z) + K_p \frac{dQ\sim_p}{dt} \tag{15}$$

where $\omega()$ is the pumping speed, K_p is the controller gain, $dQ\sim_p/dt$ is the slope calculated with available measurements of pump flow, and $Q\sim_p$ represents the measurements of the minimum pump flow in a cardiac cycle. It is worth mentioning that measurements of the minimum pump flow in three consecutive cardiac cycles are used in this work to alleviate the effect of noise on the tuning of pump speed. That is, $dQ\sim_p/dt$ is calculated with the minimum values of pump flows in three continuous cardiac cycles. In this way, the value of pump speed is recursively updated every three cardiac cycles, which is defined with z in (15).

3.4. Design of self-tuning controller

The controller in (15) adjusts the pumping speed to satisfy blood demand, but the control performance can be impacted by K_p and uncertainty. Additionally, uncertainty can introduce mismatch between the model and the failing heart managed by an LVAD. To improve control performance, an adaptive tuning rule of K_p is proposed in this work, which is described as:

$$K_p = \begin{cases} k & \text{if } dQ\sim_p/dt \geq 0 \\ k+\mu\delta & \text{if } dQ\sim_p/dt < 0 \end{cases} \tag{16}$$

where k is a fixed and patient specific controller parameter that determines the tuning rate of pumping speed to avoid suction. For example, a small k can be used for severe HF supported with an LVAD, since changes in pumping speed may result in large adjustment in pump flow, which may be harmful for the left ventricle. To find a trade-off between changes in the pump flow and the blood demand, an optimization problem is designed to optimally identify k as in:

$$\min_{\lambda=k} J = w_1 \sum_{j=1}^{R} (CO - CO_{ref})^2 + w_2 \sum_{j=1}^{R} (\Delta Var[Q_p])^2 \tag{17}$$

where λ is the decision variable, the controller gain k; and CO is the cardiac output calculated with the stochastic model of the cardiovascular-LVAD system under uncertainty, which is generated by integrating the gPC theory with the deterministic model described in Section 2. Note that CO here refers to the total outflow generated by both the pump and the native heart [14,40]. In (17), CO_{ref} is a predefined reference value of cardiac output, which is selected according to different levels of physical activities, and R is the total number of data points used in optimization (17). It is important to note that the second term in (17) calculates the changes in pump flow for all cardiac cycles used for optimization, which are computed with the higher order gPC coefficients using (14). Also, CO_{ref} can be predetermined offline based on possible activity levels of a specific subject—for example, two reference values will be required if there are two different physical activity levels, resting *vs*. mild exercise (e.g., walking stairs).

As seen in (17), the optimization penalizes the contribution of the desired perfusion demand and the change rate of pump flow to the total cost. The first term determines how to increase or decrease the pump speed to meet desired cardiac outputs (CO_{ref}), while the second term is used to prevent sudden changes in the pumping speed to ensure a safe operation of an LVAD. It is also worth mentioning that w_1 and w_2 in (17) are two weights, penalizing the contribution of each term in (17) to the total cost. These two weights are patient specific and can be selected by physicians. Based on the heart condition of a subject, these weights can be predetermined via simulations using the stochastic models and treated as fixed constants in clinical practices. For example, if the health condition of the subject is sensitive to the changes in pump speed because of a failing heart and/or its associated complications, the ratio of w_1 to w_2 can be set to a smaller value. This means a larger value of w_2 (as compared to w_1) will be used and the second term in (17) contributes significantly to the total cost, which will prevent larger changes in pump flow in consecutive cardiac cycles.

Additionally, as discussed above, it is assumed here that the PDF of R_s is known. However, it is possible that there is a mismatch between the *prior* information and the actual PDF of R_S. For example, the physiological state of HF patients may vary as patients recover, and any direct or indirect interactions of subsystems in the circulatory-LVAD system may result in changes in hemodynamics that are unknown to the modeler. In this case, the controller gain k calculated with (17) may not be the optimal value that can simultaneously satisfy the perfusion demand and avoid suction. If the nonoptimal controller gain is used, it is possible to induce suction, when the pump speed is adjusted to meet different blood needs. To address this issue, we will adjust the controller gain to quickly bring the pumping speed back to the safe operation zone. Since the sign of slope calculated with the pump flow switches from positive to negative when suction happens, it is used as an indicator to adjust the controller gain. Once a sign change has been identified, the self-tuning process will be executed. That is, the controller gain will be adaptively selected using the rules as shown in (16), i.e., $K_P = k + \mu\delta$. Details about the self-tuning rules are discussed below.

3.5. Update rules of self-tuning controller

In (16), μ is a weight to adjust the tuning rate of pump speed to avoid detrimental effects of significant changes in pump speed on the failing heart. As compared to μ, δ is the key of the self-tuning rules, which depends on the time-varying pump flow. Since uncertainty in SVR (R_S) is considered, δ is recursively updated with a stochastic model of the cardiovascular-LVAD

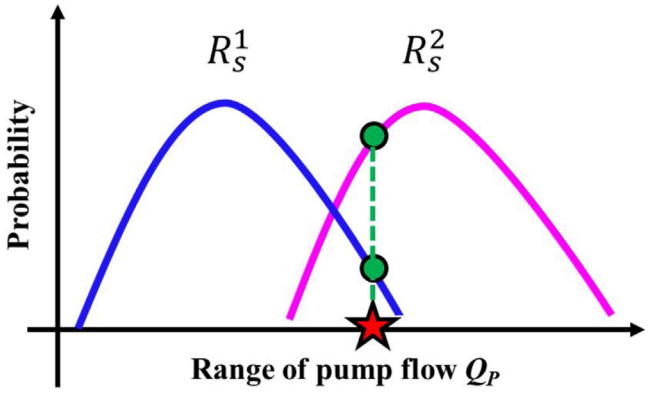

Fig. 4 – Schematic to identify the PDF of R_S with the PDF profiles of pump flow (Q_p, x_{13}).

system. The procedures to calculate δ in (16) are described as follows.

Step i: Using gPC, stochastic models of the cardiovascular-LVAD system are formulated by considering the PDF profiles of R_S, which can be obtained with offline calibration or domain knowledge [4,41].

Step ii: The gPC coefficients for each state variable in $\mathbf{x}$ (see Table 1) at the end of the systole are simulated and stored to build an offline lookup table for different mean values of R_S.

Step iii: The gPC coefficients of pump flow x_{13} obtained from the previous step are used to produce a family of PDF profiles of pump flow. Fig. 4 shows two PDF profiles of the pump flow when two different distributions of R_S are considered. When a measurement of the pump flow is available; a particular mean value of R_S can be identified using the PDF profiles of pump flow. Notably, the PDF profiles of pump flow can be estimated by generating random samples in the domain defined by ξ and by substituting them into the gPC model (9). This provides the probability distribution of pump flow over time. For simplicity, a binning algorithm, as noted in other works [42,43], is used to form the PDF of pump flow to improve computational efficiency.

Step iv: When a measurement of pump flow is available (e.g., the red star in Fig. 4), it can be referred to the PDF profiles of pump flow to infer the mean value of R_S. As seen in Fig. 4, two different probabilities (i.e., green dots) can be identified with this measurement, indicating the possibility of the patient being in specific activity level. The red star is inferred as R_s^2 due to the higher probability, indicating that the level of activity is the second mean value. This will help the controller to learn the PDF information (e.g., mean value) of SVR or R_S in Fig. 1.

Step v: Based on the identified mean value of R_S and the lookup table of gPC coefficients, the dynamic behaviors of each state variable in $\mathbf{x}$ can be predicted. Importantly, the latest

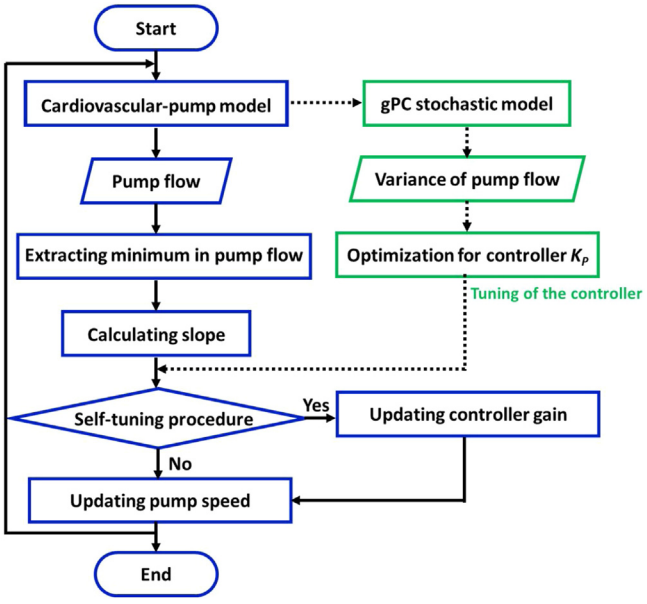

Fig. 5 – Schematic of the self-tuning feedback control of an LVAD.

pump flow measurement will be used to replace the mean value of pump flow (i.e., gPC model of pump flow) in the lookup table to calculate model predictions for each state variable in $\boldsymbol{x}$, while maintaining other coefficients unchanged.

Step vi: Using the prediction of pump flow over a finite future control horizon, the variance of pump flow can be calculated in a real time manner. The variance in pump flow is estimated with (14) using these higher order gPC coefficients in (9). To adjust the controller gain in (16), only the variance of one step ahead prediction is assigned to δ. Following this, the controller gain in (16) will be updated, once a suction has been identified. This can quickly bring the LVAD to a safe operation zone and avoid significant change in the pump speed. The efficiency of the self-tuning controller will be demonstrated in Section 4.

3.6. *Schematic of the proposed control design*

A schematic of the control algorithm for automatic tuning of the pumping speed of an LVAD is given in Fig. 5. Once the measurements of pump flow are available, the minimum values of the pump flow in three consecutive cardiac cycles will be extracted to calculate the slope in order to adjust the pumping speed.

When the slope calculated with the pump flow is found to be negative, the self-tuning procedure will be executed to update the controller parameter, so that the controller keeps the pump speed within a safe operation zone. Otherwise, the pump speed is modulated by a fixed controller to satisfy the blood needs. It is important to note that the controller gain in (16) is optimized with (17). The variation in the pump flow in (17) is recursively calculated with the stochastic model, which are highlighted in green in Fig. 5.

4. Results and discussion

4.1. *Parameters setup to describe physical activities*

Five parameters will be adjusted to describe physiological changes resulting from different physical activities based on other works [4,13,15]. For the left and right ventricles, the contractility is defined by the maximum elastance, i.e., $E_{L,max}$ and $E_{R,max}$, which were set to 1.2 and 0.56 mmHg/ml, respectively. To simulate the time-varying changes in physiological conditions, e.g., changes from resting to mild exercising, it was assumed that the elastance can increase by 20% and 25%, respectively. Further, it was assumed that the heart rate can vary between 90 and 120 bpm, depending on the physical activity of subjects—resting or mild exercise. The pulmonary vascular resistance (PVR or R_{Pm} in Fig. 1) was set to 0.06 for exercising and was decreased by 40%, when the patient is resting. Note that two different mean values were used for the systemic vascular resistance (SVR or R_S in Fig. 1), i.e., 1 mmHg/ml/s was used to describe resting, whereas 0.75 mmHg/ml/s was used for mild exercise. It is also worth mentioning that only the systemic vascular resistance in this work was defined as parametric uncertainty—approximated with (8) for algorithm illustration, but the stochastic modeling and control design can be easily extended to other uncertainties such as the heart rate, which is not discussed for brevity.

4.2. *Uncertainty propagation and formulation of gPC models*

In this work, it was assumed that SVR (or R_S) follows a normal distribution rather than a fixed constant to describe the inter- and/or intra-patient uncertainty. As noted above, two mean values were used (i.e., 1 and 0.75 mmHg/ml/s). Further, perturbations were introduced to account for uncertainty, which was equivalent to 10% changes around each of these mean values.

To build a stochastic gPC model, the first step is to rewrite SVR with a gPC expansion as shown in (8). Since uncertainty follows a normal distribution, the polynomial order q in (8) is 1. Since one uncertainty is considered, i.e., $n = 1$, and q is 1, the total number of terms to estimate each variable in Table 1 is 2, i.e., Q = 1. This implies that each variable in $\boldsymbol{x}$ will be described with 2 coupled equations, thus resulting in 26 equations in total for the stochastic cardiovascular-LVAD model. The calculation of the gPC coefficients for $\boldsymbol{x}$ follows the steps as described in Section 2. As an example, Fig. 6 shows the results for three variables defined in Table 1, the left ventricular pressure (LVP, x_{12}), aortic pressure (AoP, x_4), and pump flow (Q_P, x_{13}).

Fig. 6 shows the results of three consecutive cardiac cycles, for which the mean of R_S was set to 1 mmHg/ml/s, indicating that the patient is resting. The PVR used for simulations was 0.101 mmHg/ml/s, and the HR was set to 90 bpm. The maximum elastances of the left and right ventricles, i.e., $E_{L,max}$ and $E_{R,max}$, describing the contractility of the left and right heart, were set to 1.2 and 0.56 mmHg/ml/s, respectively. The pump speed was set to 10 krpm.

The first row in Fig. 6 shows the gPC coefficients of three aforementioned state variables, while the second row shows dynamic changes of each variable under uncertainty. Using the gPC coefficients, the upper and lower limits of each variable in $\boldsymbol{x}$ can be computed at any time point of simulations. For example, σ in the second column is the standard deviation computed with (14), using the gPC coefficients in (9), i.e., $0 < l \leq Q$. It was found that uncertainty has significant impact on the pump flow after the systole period in a cardiac cycle, see the circled region in Fig. 6(f). This provides useful information to adjust the pumping speed as discussed below. In addition, it is worth mentioning that gPC coefficients of $\boldsymbol{x}$ can be saved as an offline lookup table, which will be used to predict the dynamic behaviors of each variable over a finite future control horizon for the tuning of the controller.

4.3. *Optimization of the controller gain*

To improve control performance, it is essential to identify an optimal controller gain in (16). The optimization defined in (17) can find a trade-off between the desired cardiac output and the change rate in pumping speed. To find k, (17) was executed and solved with interior-point optimization method in Matlab with different pairs of optimization weights, i.e., w_1 and w_2 in (17). It is imporant to note that different combinatons of weights provide differnet optimization results, i.e., different values of k, which penalizes the contribution of each term in (17) to the total cost. The appropriate selction of weights is patient

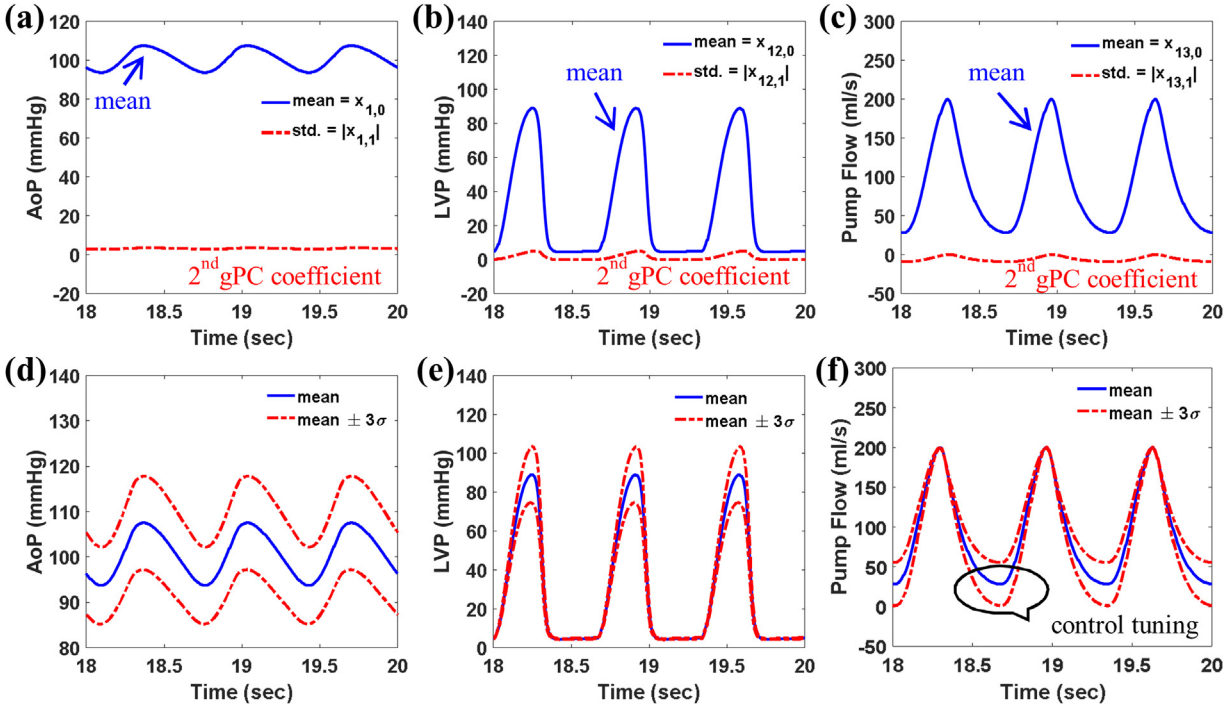

Fig. 6 – Dynamic behaviour of hemodynamic variables in Table 1 in the presence of uncertainty in R_S when the patient is resting. The first row shows the gPC coefficients of aortic pressure (AoP, x_1) in (a), the gPC coefficients of left ventricular pressure (LVP, x_{12}) in (b), and the gPC coefficients of pump flow (Q_P, x_{13}) in (c). The second row shows the mean and confidence level of model predictions, for which the aortic pressure (AoP, x_1) is shown in (d), the left ventricular pressure (LVP, x_{12}) is given in (e), and the pump flow (Q_P, x_{13}) in displayed in (f).

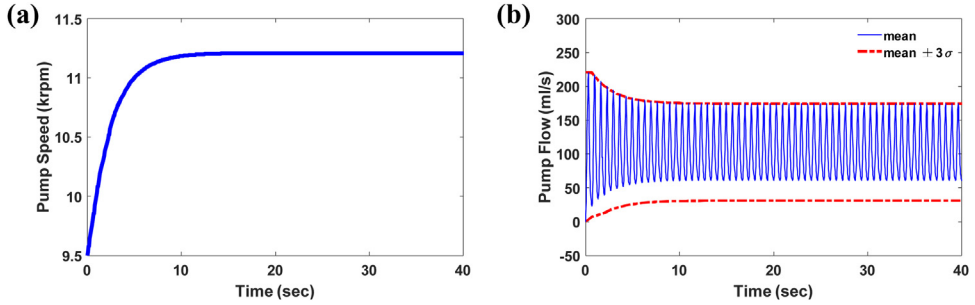

Fig. 7 – Simulations results with the feedback controller for a constant level of activity (resting): (a) controlled pump speed and (b) the corresponding pump flow with pump speed in (a).

specific. For algorithm illustration, both weights were set to 1 in (17) and the optimized result of k was found to be ~0.44. This value was further used in the following case studies. For brevity, the controller gain k obtained with different optimization weights is not shown.

4.4. *Case 1: constant physical activity*

In this case study, the activity level of an LVAD recipient was assumed to be unchanged (i.e., resting) for a period of time to ensure that the pumping speed can be adjusted properly by the controller, while avoiding suction. To describe hemodynamics when patients are resting, the HR was set to 90 bpm. The mean value of R_S and constant R_{Pm} were set to 1 and 0.101 mmHg/ml/s, respectively. Fig. 7 shows the results of the LVAD pumping speed tuned by the controller and the corresponding pump flow. Since uncertainty (R_S) is considered, Fig. 7 also displays the predicted upper and lower limits of the pump flow, which were approximated with the gPC model. The controller gain was set to 0.44, which is the optimization result obtained in previous section. The self-tuning procedure was not executed during the simulation, since the sign of the slope calculated with minimum values of pump flow remain unchanged.

As seen in Fig. 7, the pump speed is initially increased by the controller to satisfy the physiological demands, and

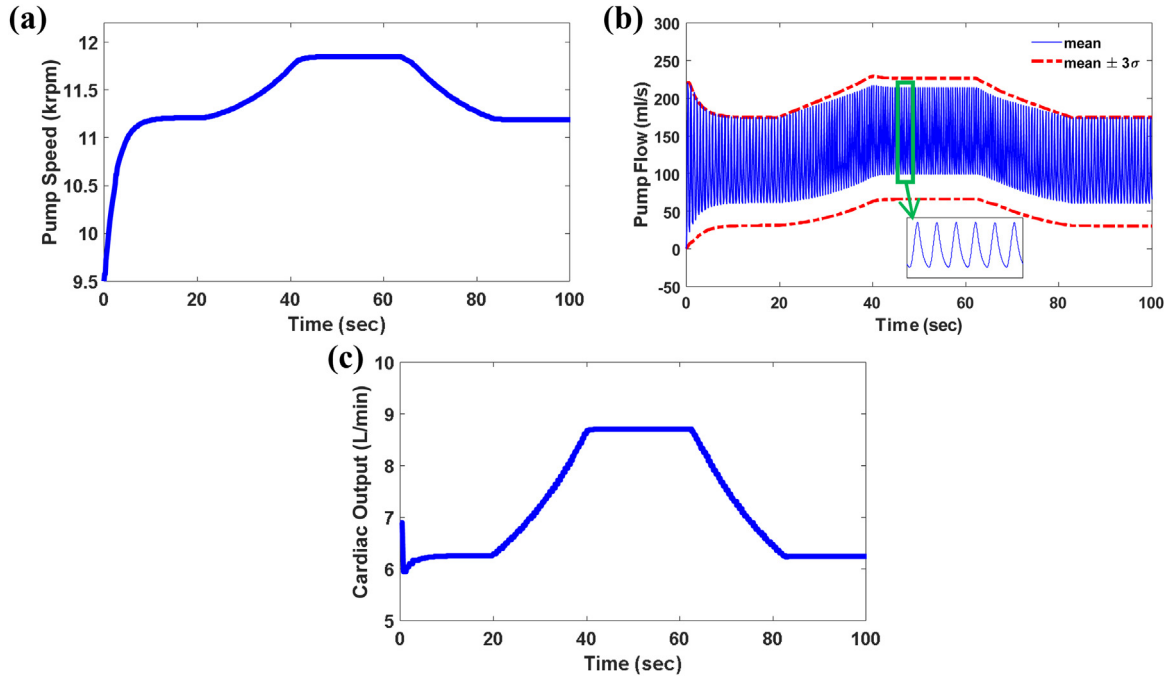

Fig. 8 – Simulations results with the feedback controller for the time-varying physical activity: (a) the controlled pumping speed, (b) the resulting pump flow and (c) the profile of cardiac outputs.

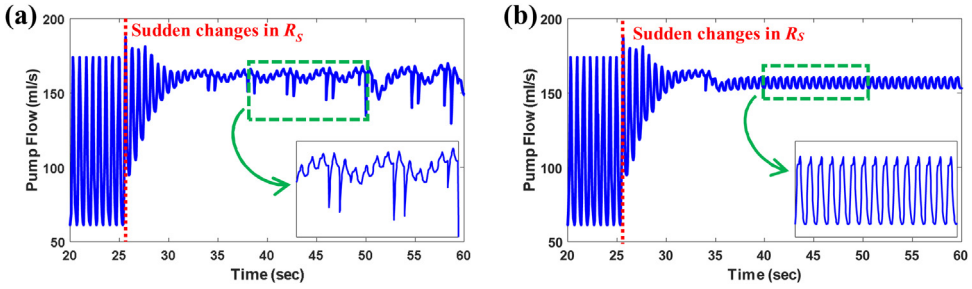

Fig. 9 – Simulation results with the feedback controller under unknown change in R_S: (a) a fixed controller gain and (b) automatically adjusted controller gain with the self-tuning procedures.

eventually stabilizes at ~1.13 × 10^4 rpm. Notably, suction can be prevented during the adjustment of the pump speed, since there are no sign switches of slope and the pulsatility of the pump flow remains unchanged. The upper and lower limits in Fig. 7 (b) represent the 99% confidence level of pump flow that is estimated with gPC coefficients.

4.5. *Case 2: time-varying physical activity*

To describe a time-varying physical activity of patients, such as switches between resting to exercising, a few assumptions were made in this case study following previous works in [4,13,15]. When a patient becomes more active, i.e., starts to do exercise from resting, the following assumptions were used: the HR was increased gradually from 90 to 120 bpm in 35 cardiac cycles, which is equivalent to approximately 20 s simulations; elastance $E_{L,max}$ and $E_{R,max}$, describing the contractility of the left ventricle and right ventricle, were increased by 20% and 25%, respectively; the SVR and PVR, i.e., R_S and R_{pm}, were decreased by 25% and 40%, respectively. Similarly, when the patient becomes less active, i.e., stops mild exercising and returns to resting, parameters used for simulations were changed back to their original values. As done in the first case study, 10% variations were introduced around each mean value of R_S to show the effect of uncertainty on the cardiovascular-LVAD system and the control performance. Also, for algorithm illustration, it was assumed that a patient was initially resting for a period of time and started to perform mild exercise for ~25 s and then gradually stopped exercising and returned back to resting. The simulation results are given in Fig. 8.

As can be observed in Fig. 8 (a), the controller can adjust the pump speed appropriately with respect to changes in physical activities to meet blood perfusion demands. Based on the

results in Fig. 8 (a), Fig. 8 (b) and (c) show the results of the pump flow and cardiac output. As seen, the pump flow was adjusted properly to ensure proper cardiac outputs without inducing any suction. Similar to the first case study, Fig. 8 (b) also shows the 99% confidence interval of the predicted pump flow under uncertainty. It is worth mentioning that we assumed in this case study that there is no mismatch between the model and the actual cardiovascular-LVAD system, i.e., the PDF of R_S is accurate. Thus, the self-tuning procedure was not executed, and the controller gain remained unchanged for the simulations shown in Fig. 8.

4.6. *Case 3: self-tuning controller under unknown changes*

It is assumed in previous case studies that the PDF of R_S is *a priori* given, i.e., the patient's health condition can be closely monitored and evaluated by physicians. In this case, depending on the physiological condition of the patient, the mean value of R_S can be identified based on the PDFs of R_S as shown in Fig. 4, and the model involved in the controller can be updated. However, as mentioned previously, it is possible that the physiological condition of HF patients changes over time. For example, anemia, hyperthermia and myocardial infraction can decrease SVR. In addition, side effects of medication such as histamine releasing drugs can also cause the blood flow resistance in the systemic circulation to decrease [44,45]. Further, it is also possible that the health condition of the heart of an LVAD recipient can become worse due to complications such as aortic insufficiency [46]. The changes in SVR can result in mismatch between the model and the actual cardiovascular-LVAD system. In this case, the controller gain solved with optimization (17) may not be the optimal controller parameter, which may result in suction and consequently deteriorate the control performance, when pump speed is adjusted. To address this, the self-tuning controller is executed to ensure a safe operation of an LVAD.

Following the discussion above, it was assumed in this case study that unknown change in R_S can happen and the self-tuning controller is automatically executed to tune the pumping speed to meet blood needs. To illustrate the efficiency, the controller with fixed controller gain was also used and compared with the self-tuning controller in terms of control performance. Fig. 9 shows the simulation results. For algorithm illustration, the value of R_S was changed from 1 to 0.65 mmHg/ml/s at ~25.3 s to describe unexpected variations that are unknown to modelers. Fig. 9 shows the simulation results of the pump flow when different controllers were used.

As can be seen in Fig. 9(a), when the fixed controller was used, the pump flow was increased due to the sudden decrease in SVR, indicating that the patient is more active than the mild exercise. This means more blood is required to satisfy perfusion demand. This subsequently increases the pumping speed to increase the pump flow. However, since the change in SVR is unknown to the modeler, the controller gain k optimized with (17) is not the optimal parameter. This consequently results in sustained suction when the pumping speed is adjusted, as seen in Fig. 9(a), since there are sign switches between the slopes computed from the pump flow data.

Compared to the fixed controller, the simulation results given in Fig. 9 b) shows that the self-tuning controller can quickly bring the pump speed back to a safe operating condition and prevent sustained suction. As can be seen in Fig. 9(b), it took about 3 s for the controller to identify a new operating condition of pump and prevent sustained suction.

5. Discussion

Our objective is to develop a stochastic model to incorporate intrinsic variability—uncertainty in systemic vascular resistance (SVR or R_S), which is related to the afterload of the left ventricle and to design a robust self-tuning controller using predictions of the stochastic model to adjust automatically the pumping power of an LVAD. Despite several models of the cardiovascular-LVAD system are available in the literature, stochastic models that can account for inter- and/or intra-variability in subjects have not been previously reported to the best of our knowledge. As a proof of concept study, the effect of uncertainty on hemodynamic of the heart was investigated, which was further used for the controller design. In the presence of uncertainty, the self-tuning controller in this work can adjust the pump speed with respect to different activity levels and can bring the controller back to the safe operating condition, when dealing with unexpected and sudden changes in R_S. This indicates the possibility to apply the self-tuning controller in clinical use since SVR of HF patients may vary over time and these changes may not be accurately and closely monitored [45,47,48].

Compared to existing control strategies of LVADs, the controller developed in this work has several unique characteristics. For example, a gain-scheduling controller was developed to tune the pumping speed using the pressure difference between the left ventricle and the aorta [6]; and a Gaussian process model was used to predict blood viscosity to adjust the pumping power [8]. A main issue of these control strategies is that the control performance can be constrained by the model uncertainty, since models are often calibrated with limited training dataset and the values of model parameters cannot be known with certainty. In this case, control performance can be deteriorated. To address this, the stochastic model of the cardiovascular-LVAD system incorporates uncertainty and provides a probabilistic description of model predictions, which will provide useful information for tuning of an LVAD. It is also worth mentioning that fuzzy logic rules were previously used for control design [6,9–11], but these methods require a reference of pulsatility or blood flow for control tuning and cannot consider variability in heart function [4], such as various stages of HF. Thus, they may not be suitable for long term clinical uses. We also would like to point out that only uncertainty in the systemic vascular resistance was studied here, but the modeling and control strategy can be easily extended to other uncertainties. In addition, to expand this work, other factors, such as different time-varying elastance functions and the effect of ventilation on an LVAD, can be investigated in the future.

6. Conclusion

In this paper, we present a deterministic cardiovascular-LVAD model, including the systemic and pulmonary circulations, to

describe the heart managed by an LVAD. The model is further integrated with the gPC theory to build a stochastic surrogate model that can efficiently evaluate the effect of uncertainty (e.g., patient heterogeneity) on physiological states (e.g., aortic pressure). Using the predictions of stochastic models, an optimization was designed to identify the optimal feedback controller parameter, which can be used to automatically adjust the pumping speed and to prevent suction. In addition, a self-tuning controller was developed to deal with unexpected mismatch between the stochastic model and the actual cardiovascular-LVAD system in order to further improve the control performance.

To show the efficacy of the proposed control algorithm, three different case studies were investigated, which mimic changes in patients' activity levels. The results show that the self-tuning controller can adjust the pumping speed to provide appropriate cardiac output with respect to different physical activities, while preventing suction. Further, it was found that the self-tuning controller can quickly adjust the pump speed and maintain an LVAD to be operated within a safe operating zone, compared to a fixed controller with constant controller parameter.

Authorship statement

All contributors who meet authorship criteria are listed as authors in this manuscript; and all authors certify that they have participate sufficiently in the work to take public responsibility for explaining the content, including participation in the concept, design, analysis, writing, and revision of the manuscript.

Each author certifies that this material in this revision has not been submitted to other journals.

Declaration of interest

The authors declare that they have no known competing financial interests or personal relationships that could have appeared to influence the work reported in this paper.

Acknowledgements

This work was supported in part by National Science Foundation (CMMI-1646664, CMMI-1728338, and CMMI-1727487).

Appendix A. Simulation results for the cardiovascular system

For model validation, Fig. A1 here shows the simulation results of the cardiovascular system in the absence of an LVAD. For both sides of the heart, nine cardiac cycles were simulated, and the last three cardiac cycles were shown in Fig. A1. For simulations in Fig. A1, heart rate (HR) was set to 90 bpm, and R_S (SVR) and R_{Pm} (PVR) were set to 1 and 0.101 mmHg/ml/s, respectively. In addition, the maximum elastance of the left and right ventricles used in the simulations was 1.2 and 0.56 mmHg/ml, respectively.

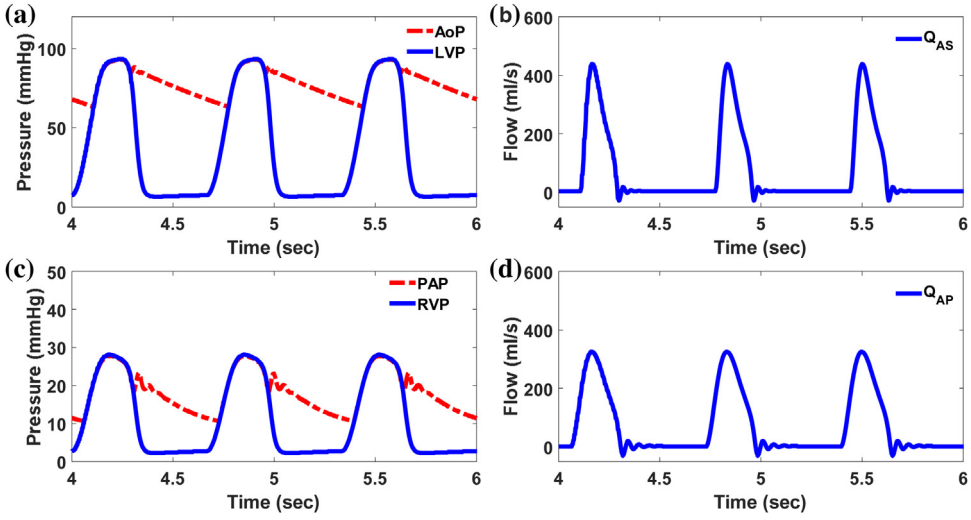

Fig. A1 – Dynamic behaviour of hemodynamic variables of a resting patient without an LVAD: (a) Aortic pressure (AoP) and left ventricular pressure (LVP), (b) Arterial systemic blood flow (Q_{AS}), (c) Pulmonary artery pressure (PAP) and right ventricular pressure (RVP), and (d) arterial pulmonary circulation blood flow (Q_{AP}).

REFERENCES

[1] Mancini D, Colombo PC. Left ventricular assist devices: a rapidly evolving alternative to transplant. J Am Coll Cardiol 2015;65(23):2542–55.
[2] Simaan MA, Ferreira A, Chen S, Antaki JF, Galati DG. A dynamical state space representation and performance analysis of a feedback-controlled rotary left ventricular assist device. IEEE Trans Control Syst Technol 2009;17(1):15–28.
[3] Shi Y, Korakianitis T, Bowles C. Numerical simulation of cardiovascular dynamics with different types of VAD assistance. J Biomech 2007;40(13):2919–33.
[4] Wu Y. Design and testing of a physiologic control system for an artificial heart pump. [Ph.D. dissertation] Mech. Aerosp. Eng.. University of Virginia; 2004.
[5] Slaughter MS, Pagani FD, Rogers JG, Miller LW, Sun B, Russell SD, et al. Clinical management of continuous-flow left ventricular assist devices in advanced heart failure. J Heart Lung Transplant 2010;29(4):S1–39.
[6] Wang Y, Koenig SC, Slaughter MS, Giridharan GA. Rotary blood pump control strategy for preventing left ventricular suction. ASAIO J 2015;61(1):21–30.
[7] Ohuchi K, Kikugawa D, Takahashi K, Uemura M, Nakamura M, Murakami T, et al. Control strategy for rotary blood pumps. Artif Organs 2001;25(5):366–70.
[8] Petrou A, Kanakis M, Boës S, Pergantis P, Meboldt M, Daners MS. Viscosity prediction in a physiologically controlled ventricular assist device. IEEE Trans Biomed Eng 2018;65 (10):2355–64.
[9] Choi S, Antaki JE, Boston R, Thomas D. A sensorless approach to control of a turbodynamic left ventricular assist system. IEEE Trans Control Syst Technol 2001;9 (3):473–82.
[10] Choi S, Boston JR, Antaki JF. Hemodynamic controller for left ventricular assist device based on pulsatility ratio. Artif Organs 2007;31(2):114–25.
[11] Fu M, Xu L. Computer simulation of sensorless fuzzy control of a rotary blood pump to assure normal physiology. ASAIO J 2000;46(3):273–8.
[12] Martina J, de Jonge N, Rutten M, Kirkels JH, Klöpping C, Rodermans B, et al. Exercise hemodynamics during extended continuous flow left ventricular assist device support: the response of systemic cardiovascular parameters and pump performance. Artif Organs 2013;37(9):754–62.
[13] AlOmari AH, Savkin AV, Stevens M, Mason DG, Timms DL, Salamonsen RF, et al. Developments in control systems for rotary left ventricular assist devices for heart failure patients: a review. Physiol Meas 2012;34(1):R1–27.
[14] Ferreira A. A rule-based controller based on suction detection for rotary blood pumps. [Ph.D. dissertation] Dept. Elect. Comput. Eng.. University of Pittsburgh; 2007.
[15] Stevens MC, Wilson S, Bradley A, Fraser J, Timms D. Physiological control of dual rotary pumps as a biventricular assist device using a master/slave approach. Artif Organs 2014;38(9):766–74.
[16] Son J, Du D, Du Y. Stochastic modeling and control of circulatory system with a left ventricular assist device. 2019 American Control Conference (ACC). IEEE; 2019. p. 5408–13.
[17] Eck VG, Feinberg J, Langtangen HP, Hellevik LR. Stochastic sensitivity analysis for timing and amplitude of pressure waves in the arterial system. Int J Numer Meth Biomed Eng 2015;31(4):e02711.
[18] Huberts W, Donders WP, Delhaas T, van de Vosse FN. Applicability of the polynomial chaos expansion method for personalization of a cardiovascular pulse wave propagation model. Int J Numer Meth Biomed Eng 2014;30 (12):1679–704.
[19] Quicken S, Donders WP, van Disseldorp EMJ, Gashi K, Mees BME, van de Vosse FN, et al. Application of an adaptive polynomial chaos expansion on computationally expensive three-dimensional cardiovascular models for uncertainty quantification and sensitivity analysis. J Biomech Eng 2016;138(12):121010.
[20] Hu Z, Du D, Du Y. Generalized polynomial chaos-based uncertainty quantification and propagation in multi-scale modeling of cardiac electrophysiology. Comput Biol Med 2018;102:57–74.
[21] Du Y, Budman H, Duever TA. Comparison of stochastic fault detection and classification algorithms for nonlinear chemical processes. Comput Chem Eng 2017;106:57–70.
[22] Xiu D. Numerical methods for stochastic computations: a spectral method approach. Princeton, NJ, USA: Princeton University Press; 2010.
[23] Avanzolini G, Barbini P, Cappello A, Cevenini G. CADCS simulation of the closed-loop cardiovascular system. Int J Biomed Comput 1988;22(1):39–49.
[24] Fernandez de Canete J, Del Saz-Orozco P, Moreno-Boza D, Duran-Venegas E. Object-oriented modeling and simulation of the closed loop cardiovascular system by using SIMSCAPE. Comput Biol Med 2013;43(4):323–33.
[25] Shi Y, Korakianitis T. Numerical simulation of cardiovascular dynamics with left heart failure and in-series pulsatile ventricular assist device. Artif Organs 2006;30(12):929–48.
[26] Korakianitis T, Shi Y. A concentrated parameter model for the human cardiovascular system including heart valve dynamics and atrioventricular interaction. Med Eng Phys 2006;28(7):613–28.
[27] Korakianitis T, Shi Y. Numerical simulation of cardiovascular dynamics with healthy and diseased heart valves. J Biomech 2006;39(11):1964–82.
[28] Suga H, Sagawa K, Shoukas AA. Load independence of the instantaneous pressure-volume ratio of the canine left ventricle and effects of epinephrine and heart rate on the ratio. Circ Res 1973;32(3):314–22.
[29] Suga H, Sagawa K. Instantaneous pressure-volume relationships and their ratio in the excised, supported canine left ventricle. Circ Res 1974;35(1):117–26.
[30] Vandenberghe S, Segers P, Steendijk P, Meyns B, Dion RAE, Antaki JF, et al. Modeling ventricular function during cardiac assist: does time-varying elastance work? ASAIO J 2006;52(1):4–8.
[31] Stergiopulos N, Meister JJ, Westerhof N. Determinants of stroke volume and systolic and diastolic aortic pressure. Amer J Physiol 1996;270(6):H2050–9.
[32] Choi S, Boston JR, Thomas D, Antaki JF. Modeling and identification of an axial flow blood pump. Proceedings of the 1997 American Control Conference (Cat. No.97CH36041). IEEE; 1997. p. 3714–5.
[33] Xiu D, Karniadakis GE. The Wiener–Askey polynomial chaos for stochastic differential equations. SIAM J Sci Comput 2002;24(2):619–44.
[34] Moazami N, Fukamachi K, Kobayashi M, Smedira NG, Hoercher KJ, Massiello A, et al. Axial and centrifugal continuous-flow rotary pumps: a translation from pump mechanics to clinical practice. J Heart Lung Transplant 2013;32(1):1–11.
[35] Schwarz KQ, Parikh SS, Chen X, Farrar DJ, Steinmetz S, Ramamurthi S, et al. Non-invasive flow measurement of a rotary pump ventricular assist device using quantitative contrast echocardiography. J Am Soc Echocardiogr 2010;23 (3):324–9.
[36] Trinquero P, Pirotte A, Gallagher LP, Iwaki KM, Beach C, Wilcox JE. Left ventricular assist device management in the emergency department. West J Emerg Med 2018;19 (5):834–41.

[37] Ferreira A, Boston JR, Antaki JF. A control system for rotary blood pumps based on suction detection. IEEE Trans Biomed Eng 2009;56(3):656–65.
[38] Gwak KW. Application of extremum seeking control to turbodynamic blood pumps. ASAIO J 2007;53(4):403–9.
[39] Konishi H, Antaki JF, Amin DV, Boston JR, Kerrigan JP, Mandarino WA, et al. Controller for an axial flow blood pump. Artif Organs 1996;20(6):618–20.
[40] Shi Y, Brown AG, Lawford PV, Arndt A, Nuesser P, Hose DR. Computational modelling and evaluation of cardiovascular response under pulsatile impeller pump support. Interface Focus 2011;1(3):320–37.
[41] Bartoli CR, Dowling RD. The future of adult cardiac assist devices: novel systems and mechanical circulatory support strategies. Cardiol Clin 2011;29(4):559–82.
[42] Son J, Du Y. Model-based stochastic fault detection and diagnosis of lithium-ion batteries. Processes 2019;7(1):38.
[43] Du Y, Duever TA, Budman H. Fault detection and diagnosis with parametric uncertainty using generalized polynomial chaos. Comput Chem Eng 2015;76:63–75.
[44] Saini V, Samra T. Persistent postoperative hypercyanotic spells in an adult with surgically untreated tetralogy of fallot: use of ketamine infusion. J Anaesthesiol Clin Pharmacol 2017;33(3):412–3.
[45] Melo J, Peters JI. Low systemic vascular resistance: differential diagnosis and outcome. Crit Care 1999;3(3):71–7.
[46] Jorde UP, Uriel N, Nahumi N, Bejar D, Gonzalez-Costello J, Thomas SS, et al. Prevalence, significance, and management of aortic insufficiency in continuous flow left ventricular assist device recipients. Circ Heart Fail 2014;7 (2):310–9.
[47] Reddy YNV, Melenovsky V, Redfield MM, Nishimura RA, Borlaug BA. High-output heart failure: a 15-year experience. J Am Coll Cardiol 2016;68(5):473–82.
[48] Wong M, Toh L, Wilson A, Rowley K, Karschimkus C, Prior D, et al. Reduced arterial elasticity in rheumatoid arthritis and the relationship to vascular disease risk factors and inflammation. Arthritis Rheum 2003;48(1):81–9.